ChemComm

COMMUNICATION

View Article Online
View Journal | View Issue





Cite this: *Chem. Commun.*, 2021, 57, 11189

Received 21st August 2021,
Accepted 1st October 2021

DOI: 10.1039/d1cc04669a

rsc.li/chemcomm

# Photochemistry and *in vitro* anticancer activity of Pt(IV)Re(I) conjugates†

Zhouyang Huang,[a] A. Paden King,[a] James Lovett,[b] Barry Lai,[c] Joshua J. Woods,[ad] Hugh H. Harris[b] and Justin J. Wilson*[a]

**The photophysical and photochemical properties of two Pt(IV)Re(I) conjugates were studied *via* both experimental and computational methods. Both conjugates exhibit modest photocytotoxicity against ovarian cancer cells. X-ray fluorescence microscopy showed that Pt and Re colocalize in cells whether they had been irradiated or not. This work demonstrates the potential of photoactivated multimetallic agents for combating cancer.**

Recently, Re(I) tricarbonyl ($Re(CO)_3$) complexes have gained significant attention as alternatives to conventional Pt(II) chemotherapeutics.[1–4] These compounds operate *via* mechanisms of action distinct from the covalent DNA-binding pathways that are operative for Pt(II) complexes.[5–11] For instance, our group has shown that a series of tricarbonyl rhenium isonitrile polypyridyl (TRIP) complexes exhibit potent *in vitro* anticancer activity by inducing endoplasmic reticulum (ER) stress.[12–14]

Given the potential for distinct mechanisms of action afforded by different metal centers, there has been a growing interest in developing heterometallic complexes as dual-action anticancer agents.[15,16] Despite the clinical success of Pt compounds and the arising promise of cytotoxic $Re(CO)_3$ complexes, there are only four studies that investigate the anticancer activities of heterometallic Pt–Re conjugates;[17] three of them explored Pt(II)Re(I) complexes[18–20] and the fourth studied a Pt(IV)Re(I) nanoparticle-based system.[21] We sought to prepare and investigate molecular conjugates comprising TRIP and a Pt(IV) prodrug, which can be activated by reduction in cancer cells to release a biologically active Pt(II) complex. The pharmacological properties of Pt(IV) prodrugs can be enhanced by employing bioactive ligands that can kill cancer cells *via* a complementary mechanism of action, affording dual-action drug candidates.[22–24]

To prepare Pt(IV)-TRIP conjugates, we synthesized **TRIP-NH$_2$** (Scheme S1, ESI†), which contains an amine group that can be used for the construction of stable amide bonds. Coupling of **TRIP-NH$_2$** with succinate-containing Pt(IV) analogues of cisplatin and oxaliplatin afforded two amide-linked trimetallic conjugates, **CisPtRe** and **OxaliPtRe** (Scheme S2, ESI† and Chart 1).[25,26] We also synthesized the monometallic Re compound **TRIP-suc** (Chart 1), which serves as the axial ligand for **CisPtRe** and **OxaliPtRe**. All four complexes were characterized by multinuclear NMR spectroscopy, mass spectrometry, infrared spectroscopy, and HPLC (Fig. S1–S11, ESI†). The stability of **CisPtRe** and **OxaliPtRe** under physiologically relevant conditions was assessed by HPLC. After 24 h at 37 °C, both complexes remain >80% intact in pH 7.4 phosphate-buffered saline (PBS) (Fig. S12, ESI†). In the presence of 20 fold excess glutathione (GSH), an intracellular reducing agent that is known to activate Pt(IV) prodrugs,[27] 35% of **CisPtRe** was reduced after 24 h, triggering the release of the axial **TRIP-suc** ligand (Fig. S13, ESI†). By contrast, only of a trace amount of **OxaliPtRe** was reduced under these same conditions, indicating that this compound is significantly more stable to chemical reduction. The enhanced stability of oxaliplatin-based Pt(IV) carboxylate complexes to reduction has been previously noted.[28] The photophysical

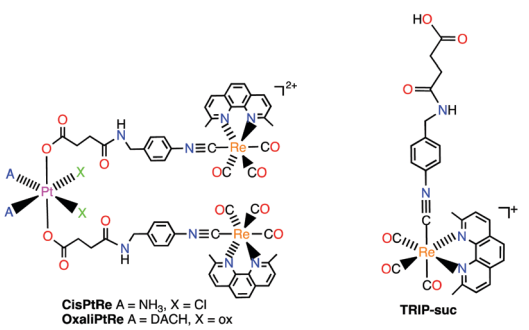


Chart 1 Structures of **CisPtRe**, **OxaliPtRe** and **TRIP-suc**.

[a] *Department of Chemistry and Chemical Biology, Cornell University, Ithaca, NY 14853, USA. E-mail: jjw275@cornell.edu*
[b] *Department of Chemistry, The University of Adelaide, South Australia 5005, Australia*
[c] *Advanced Photon Source, X-ray Science Division, Argonne National Laboratory, Argonne, IL 60439, USA*
[d] *Robert F. Smith School for Chemical and Biomolecular Engineering, Cornell University, Ithaca, NY 14853, USA*

† Electronic supplementary information (ESI) available. See DOI: 10.1039/d1cc04669a

properties of **CisPtRe**, **OxaliPtRe**, and **TRIP-suc** are described in Table 1 and Fig. S19 and S20, ESI.†

We next sought to investigate the photochemistry of **CisPtRe** and **OxaliPtRe**. Irradiation of these two conjugates with 365 nm light for 24 h at 37 °C triggered their complete decomposition, yielding **TRIP-suc** as the major HPLC-detectable product (Fig. S14, ESI†). To further characterize the photoproducts of this reaction, we monitored a dimethylsulfoxide (DMSO) solution of **CisPtRe** by $^{195}$Pt NMR spectroscopy as it was photolyzed with 365 nm light. Over the course of this irradiation, the $^{195}$Pt NMR resonance of **CisPtRe** at 1221 ppm disappeared with the concomitant appearance of a new resonance at −3449 ppm (Fig. S17, ESI†). This chemical shift is consistent with well-characterized Pt(II) DMSO complexes,[29–31] thus suggesting that irradiation of **CisPtRe** causes reduction of the Pt(IV) center. For **OxaliPtRe**, the production of the Pt(II) product oxaliplatin upon photolysis was directly detected by $^{1}$H NMR spectroscopy, validating that photoreduction of the Pt(IV) center occurs for this complex as well (Fig. S18, ESI†). Importantly, the photoreduction of both **CisPtRe** and **OxaliPtRe** proceeds much faster than the thermal reduction by GSH under the same condition (Fig. S13, ESI†), suggesting that these complexes could be photoactivated under biological conditions. In addition to the photoreduction of the Pt(IV) center, **TRIP-suc**, which is released during this process, also undergoes further photodecomposition, albeit on a slower timescale (Fig. S15, ESI†). ESI-MS analysis of the photoreaction of **TRIP-suc** revealed the presence of a Re(I) dicarbonyl ($Re(CO)_2$) species (Fig. S16, ESI†). Moreover, the IR spectrum of the photoproduct (Fig. S15, ESI†) shows two CO stretching modes at 1921 and 1866 cm$^{-1}$, values that are significantly lower than those found in $Re(CO)_3$ complexes, but are consistent with well characterized $Re(CO)_2$ complexes.[32–34] These results suggest that the photolysis of **TRIP-suc** leads to CO dissociation, a phenomenon that has been observed in other $Re(CO)_3$ isonitrile complexes.[35] The CO released from the secondary photolysis of **TRIP-suc** could elicit additional cytotoxic effects, potentiating the photoinduced anticancer activity of these complexes.[36] The quantum yield for the CO dissociation from **TRIP-suc** is 4.3% (Table 1 and Fig. S21, ESI†). The photoreduction of **CisPtRe** proceeds with a much higher quantum yield (13.0%) than **OxaliPtRe** (2.1%) (Table 1, Fig. S22 and S23, ESI†). This trend is consistent with relative rates of thermal reduction for both complexes (Fig. S13, ESI†).

To gain a deeper understanding of the photochemical behavior of these compounds, we performed density functional theory (DFT) and time-dependent DFT (TD-DFT) calculations. The frontier molecular orbitals (FMOs) of **CisPtRe**, **OxaliPtRe** and **TRIP-suc** are shown in Fig. 1. The HOMO of **TRIP-suc** and HOMO and HOMO−1 of the Pt(IV)Re(I) conjugates are at the same energy and can be primarily described as a "$t_{2g}$-like" set of Re d orbitals engaged in π backbonding with the CO and CN ligands. Likewise, the LUMO and LUMO+1 of **TRIP-suc**, π* orbitals of the diimine (NN) ligands, are at the same energies as the LUMO+2 to LUMO+5 of the Pt(IV)Re(I) conjugates, which are also ligand-based π* orbitals. These results suggest that conjugation of **TRIP-suc** to the Pt(IV) fragments does not significantly perturb its electronic structure. Experimentally, this conclusion is further supported by the similar photophysical and NMR spectroscopic properties of **TRIP-suc** and the conjugates (Fig. S2–S4 and S19, ESI†). The main difference between the FMOs of the Pt(IV)Re(I) conjugates and **TRIP-suc** is the presence of unoccupied "$e_g$-like" Pt-based d σ* orbitals (LUMO and LUMO+1) that reside energetically between the empty diimine π* (LUMO+2, LUMO+3) and occupied d orbitals (HOMO, HOMO−1) of **TRIP-suc**. The presence of these Pt-based d orbitals gives rise to additional excited states that reside lower in energy than the optically active MLCT state of TRIP-suc, as calculated by TD-DFT (Fig. S28, ESI†). Of significance to the experimentally observed photoreduction pathways of **CisPtRe** and **OxaliPtRe**, several of these intermediary excited states have metal-to-metal charge transfer (MMCT) character, whereby an electron transitions from the Re "$t_{2g}$-like" d orbital into a Pt "$e_g$-like" σ* orbital. Although these MMCT excited states have very low oscillator strengths and are not likely to be directly accessed *via* irradiation with light, population of the high oscillator strength MLCT states of **TRIP-suc** by photoexcitation followed by photoinduced electron transfer to these MMCT states is energetically viable. Because these MMCT excited states require population of Pt σ* orbital, dissociation of the axial **TRIP-suc** ligands, as observed experimentally, will occur. Assuming that this electron transfer occurs in the "non-inverted Marcus region",[37] the lower photoreduction quantum yield of **OxaliPtRe** compared to **CisPtRe** is consistent with our DFT calculations, which show that there is a smaller energy gap between the MMCT and MLCT states of the former and

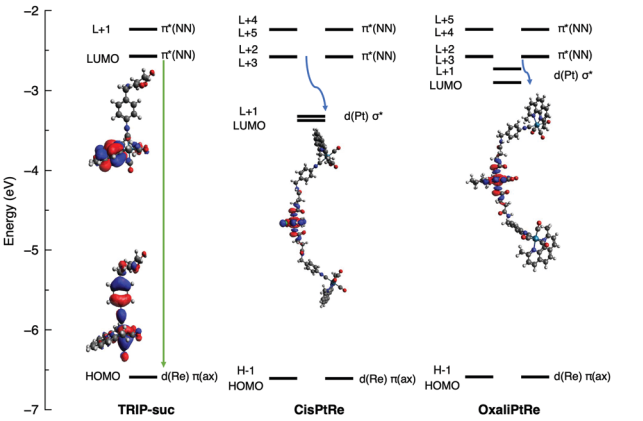


Fig. 1 Frontier molecular orbital diagram of **TRIP-suc** (left), **CisPtRe** (middle), and **OxaliPtRe** (right). The isodensity surface plots of the molecular orbitals are provided in Fig. S25–S27, ESI.† Green arrow: electronic transition involved in phosphorescence from the Re(I)-based $^{3}$MLCT excited state. Blue curved arrows: electronic transitions involved in photoinduced electron transfer from the diimine π* to the Pt(IV) σ* orbital.

Table 1 Photophysical properties of **CisPtRe**, **OxaliPtRe** and **TRIP-suc**

| Compound | $\varepsilon_{365nm}$, M$^{-1}$ cm$^{-1}$ | $\Phi_{lum}$, % | $\Phi_{rxn}$, % | $\tau_{air}$ (μs) | $\tau_{N2}$ (μs) |
|---|---|---|---|---|---|
| **CisPtRe** | 3300 ± 300 | 0.4 ± 0.01 | 13.0 ± 0.6 | 1.0 | 2.2 |
| **OxaliPtRe** | 3900 ± 100 | 1.8 ± 0.1 | 2.1 ± 0.1 | 0.7 | 1.1 |
| **TRIP-suc** | 1700 ± 400 | 3.4 ± 0.3 | 4.3 ± 0.5 | 1.4 | 5.3 |

therefore lower thermodynamic driving force for electron transfer. Finally, the trend in photoluminescent quantum yields ($\Phi_{lum}$ (**CisPtRe**) < $\Phi_{lum}$ (**OxaliPtRe**) < $\Phi_{lum}$ (**TRIP-suc**)) could also be explained by the fact that **CisPtRe** can undergo non-radiative decay more favorably due to a stronger thermodynamic driving force of photoinduced electron transfer, which diminishes phosphorescence. Cyclic voltammetry of **CisPtRe** and **OxaliPtRe** (Fig. S24, ESI†) shows only a minor difference in their measured irreversible peak potentials ($E_p$ = −0.99 V and −0.94 V, respectively). Although this result appears to contradict the computational studies, the interpretation of irreversible peak potentials in the context of thermodynamic reduction potentials should be approached with caution because they may reflect the overpotential required for a slow electron transfer step. In any case, the chlorides of **CisPtRe** act as bridging ligands to facilitate efficient inner sphere electron transfer, whereas the lack of such bridging ligands on **OxaliPtRe**, contributes to its slower electron transfer reactivity.[27,28]

We next evaluated the cytotoxicity of these compounds in wild-type (A2780) and cisplatin-resistant (A2780CP70) ovarian cancer cell lines in the absence and presence of 365 nm light (Table 2 and Fig. S29–S31, ESI†). In the dark, **CisPtRe** and **OxaliPtRe** exhibit modest anticancer activity in both cell lines, but are 2–3 fold less active in the A2780CP70 cells, suggesting that they are cross-resistant with cisplatin. By contrast, **TRIP-suc** is non-toxic in the absence of light. Based on the lack of cytotoxicity of **TRIP-suc** and their platinum-cross resistance, it is likely that their biological activities are mediated primarily by the Pt(IV) center. Upon irradiation with 365 nm light, a 2–3 fold enhancement in cytotoxicity against A2780 cells for both conjugates is observed. Within the cisplatin-resistant A2780CP70 cell line, however, only **OxaliPtRe** undergoes an increase in cytotoxicity upon irradiation. Thus, these two conjugates show mixed results when investigated as photoactivated drug candidates, highlighting that additional factors, such as premature chemical reduction, may be operative.

Finally, we examined uptake and intracellular distribution of **OxaliPtRe** in HeLa cervical cancer cells using X-ray fluorescence (XRF) imaging. Pt and Re in treated cells colocalize in non-nuclear, presumably cytoplasmic, regions, irrespective of whether or not a UV irradiation step was included in the incubation period (Fig. 2 and Fig. S32–S34, ESI†). The colocalization of Pt and Re in the irradiated cells is perhaps surprising given the observation noted above regarding decomposition of the conjugate as a result of irradiation in aqueous buffer. However, the photoconversion in biological media may be less efficient due to protein binding, leading to only partial photodecomposition in the cells, and perhaps more importantly, the cells may rapidly process and compartmentalize the intact conjugate prior to decomposition, providing an alternative mechanism to explain the colocalization. A more detailed discussion on the XRF studies is included in ESI.†

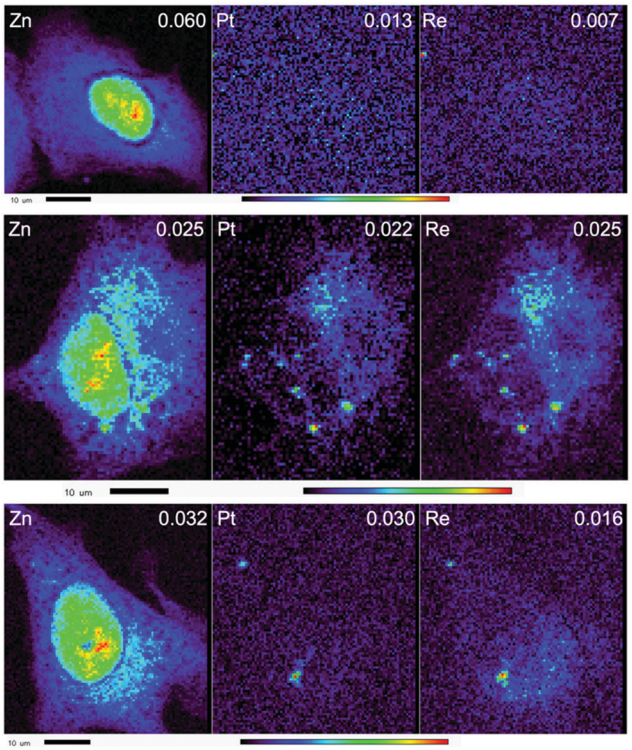


Fig. 2 X-ray fluorescence elemental distribution maps (Zn, Pt and Re) of: (top) untreated HeLa cells; (middle) HeLa cells treated with 8.5 μM **OxaliPtRe** in media in the dark for 7 h; (bottom) HeLa cells treated with 8.5 μM **OxaliPtRe** in media for 7 h, including irradiation at 365 nm for 1 h, starting 3 h into the treatment. The maximal elemental area density (units of μg cm$^{-2}$) is given in each map. The nucleus is evident in the zinc-rich region of each cell.

Table 2 $IC_{50}$ values (μM) in A2780 (ovarian) and A2780CP70 (ovarian cisplatin-resistant) cancer cells in the absence and presence of 365 nm light

| | A2780 | | | A2780CP70 | |
|---|---|---|---|---|---|
| Compound | Dark | Light[a] | PI[b] | Dark | Light |
| **CisPtRe** | 8.9 ± 3.8 | 4.8 ± 1.3 | 1.8 | 17 ± 5.0 | 24 ± 2.3 |
| **OxaliPtRe** | 9.7 ± 2.2 | 2.8 ± 0.9 | 3.5 | 27 ± 2.4 | 13 ± 5.6 |
| **TRIP-suc** | >100 | 26 ± 2.2 | 3.8 | >100 | 99 ± 15 |
| Cisplatin | 1.9 ± 0.5 | | | 19 ± 3.8 | |
| Oxaliplatin | 4.1 ± 1.4 | | | 9.3 ± 4.3 | |

[a] For light-irradiated samples, an irradiation time 1 h with 365 nm light at a photon flux (2.38 ± 0.31) × 10$^{-10}$ Einstein/s was employed. [b] Phototoxic index (PI) is the dark $IC_{50}$ value divided by the light $IC_{50}$ value.

In conclusion, we have reported the synthesis, characterization, and photophysical studies of two Pt(IV)Re(I) conjugates. Both compounds are activated *via* photoreduction with 365 nm light, releasing bioactive Pt(II) and Re(I) complexes. In comparison to other photoactivated Pt(IV) prodrugs,[38–40] the modest phototoxicity of the Pt(IV)Re(I) conjugates in this study could possibly be a consequence of their limited thermal stability and low photochemical quantum yields. The photochemical quantum yields measured in buffer may not reflect their actual photochemical conversion efficiencies in biological media, where binding to or decomposition by proteins may lead to unexpected outcomes. Furthermore, compared to photoactivated Pt(IV) complexes with bioactive axial ligands,[41,42] the axial fragments in these Pt(IV)Re(I) conjugates, **TRIP-suc**, only exhibits modest dark and light toxicity,

thus indicating that the cytotoxic effects of these trimetallic compounds are primarily from the Pt center. Additionally, compared to other multimetallic complexes that are more potent than cisplatin *in vitro*, Pt(IV)Re(I) conjugates in this work do not outperform the aforementioned classical chemotherapeutic agent.[43–46] Despite these drawbacks, these compounds still demonstrate the viability of combining different metal centers to leverage their distinct photophysical properties for accessing new photochemical activation pathways, strategies that may be of significant use for the development of new phototoxic drug candidates.

This work was supported in part by the College of Arts and Sciences at Cornell University. This work made use of the NMR facility at Cornell University, which is in-part supported by the NSF under award number CHE-1531632. This research used resources of the Advanced Photon Source, a U.S. Department of Energy (DOE) Office of Science User Facility operated for the DOE Office of Science by Argonne National Laboratory under Contract No. DE-AC02-06CH11357. HHH acknowledges support from an Australian Research Council Discovery Project (DP210102148). We thank Prof. Peng Chen and Prof. Warren Zipfel (Cornell University) for providing access to a fluorimeter and for assisting with the photoluminescence decay lifetime measurement, respectively.

## Conflicts of interest

There are no conflicts to declare.

## Notes and references

1 A. Leonidova and G. Gasser, *ACS Chem. Biol.*, 2014, **9**, 2180–2193.
2 L. C.-C. Lee, K.-K. Leung and K. K.-W. Lo, *Dalton Trans.*, 2017, **46**, 16357–16380.
3 E. B. Bauer, A. A. Haase, R. M. Reich, D. C. Crans and F. E. Kühn, *Coord. Chem. Rev.*, 2019, **393**, 79–117.
4 P. Collery, D. Desmaele and V. Veea, *Curr. Pharm. Des.*, 2019, **25**, 3306–3322.
5 I. Kitanovic, S. Can, H. Alborzinia, A. Kitanovic, V. Pierroz, A. Leonidova, A. Pinto, B. Spingler, S. Ferrari, R. Molteni, A. Steffen, N. Metzler-Nolte, S. Wölfl and G. Gasser, *Chem. – Eur. J.*, 2014, **20**, 2496–2507.
6 S. Imstepf, V. Pierroz, R. Rubbiani, M. Felber, T. Fox, G. Gasser and R. Alberto, *Angew. Chem., Int. Ed.*, 2016, **55**, 2792–2795.
7 P. V. Simpson, I. Casari, S. Paternoster, B. W. Skelton, M. Falasca and M. Massi, *Chem. – Eur. J.*, 2017, **23**, 6518–6521.
8 K. M. Knopf, B. L. Murphy, S. N. MacMillan, J. M. Baskin, M. P. Barr, E. Boros and J. J. Wilson, *J. Am. Chem. Soc.*, 2017, **139**, 14302–14314.
9 M. König, D. Siegmund, L. J. Raszeja, A. Prokop and N. Metzler-Nolte, *MedChemComm*, 2018, **9**, 173–180.
10 M. Muñoz-Osses, F. Godoy, A. Fierro, A. Gómez and N. Metzler-Nolte, *Dalton Trans.*, 2018, **47**, 1233–1242.
11 L. He, Z.-Y. Pan, W.-W. Qin, Y. Li, C.-P. Tan and Z.-W. Mao, *Dalton Trans.*, 2019, **48**, 4398–4404.
12 A. P. King, S. C. Marker, R. V. Swanda, J. J. Woods, S.-B. Qian and J. J. Wilson, *Chem. – Eur. J.*, 2019, **25**, 9206–9210.
13 S. C. Marker, A. P. King, R. V. Swanda, B. Vaughn, E. Boros, S.-B. Qian and J. J. Wilson, *Angew. Chem., Int. Ed.*, 2020, **59**, 13391–13400.
14 S. C. Marker, A. P. King, S. Granja, B. Vaughn, J. J. Woods, E. Boros and J. J. Wilson, *Inorg. Chem.*, 2020, **59**, 10285–10303.
15 V. Fernández-Moreira and M. C. Gimeno, *Chem. – Eur. J.*, 2018, **24**, 3345–3353.
16 A. van Niekerk, P. Chellan and S. F. Mapolie, *Eur. J. Inorg. Chem.*, 2019, 3432–3455.
17 Z. Huang and J. J. Wilson, *Eur. J. Inorg. Chem.*, 2021, 1312–1324.
18 N. Margiotta, N. Denora, S. Piccinonna, V. Laquintana, F. M. Lasorsa, M. Franco and G. Natile, *Dalton Trans.*, 2014, **43**, 16252–16264.
19 L. Quental, P. Raposinho, F. Mendes, I. Santos, C. Navarro-Ranninger, A. Alvarez-Valdes, H. Huang, H. Chao, R. Rubbiani, G. Gasser, A. G. Quiroga and A. Paulo, *Dalton Trans.*, 2017, **46**, 14523–14536.
20 B. Bertrand, C. Botuha, J. Forté, H. Dossmann and M. Salmain, *Chem. – Eur. J.*, 2020, **26**, 12846–12861.
21 E. Gabano, L. do Quental, E. Perin, F. Silva, P. Raposinho, A. Paulo and M. Ravera, *Inorganics*, 2017, **6**, 4.
22 D. Gibson, *Dalton Trans.*, 2016, **45**, 12983–12991.
23 D. Gibson, *J. Inorg. Biochem.*, 2021, **217**, 111353.
24 Z. Xu, Z. Wang, Z. Deng and G. Zhu, *Coord. Chem. Rev.*, 2021, **442**, 213991.
25 M. R. Reithofer, S. M. Valiahdi, M. A. Jakupec, V. B. Arion, A. Egger, M. Galanski and B. K. Keppler, *J. Med. Chem.*, 2007, **50**, 6692–6699.
26 J. J. Wilson and S. J. Lippard, *Chem. Rev.*, 2014, **114**, 4470–4495.
27 E. Wexselblatt and D. Gibson, *J. Inorg. Biochem.*, 2012, **117**, 220–229.
28 J. Z. Zhang, E. Wexselblatt, T. W. Hambley and D. Gibson, *Chem. Commun.*, 2012, **48**, 847–849.
29 B. M. Still, P. G. A. Kumar, J. R. Aldrich-Wright and W. S. Price, *Chem. Soc. Rev.*, 2007, **36**, 665–686.
30 S. J. S. Kerrison and P. J. Sadler, *Inorg. Chim. Acta*, 1985, **104**, 197–201.
31 S. J. S. Kerrison and P. J. Sadler, *J. Chem. Soc., Chem. Commun.*, 1977, 861–863.
32 C.-C. Ko, L. T.-L. Lo, C.-O. Ng and S.-M. Yiu, *Chem. – Eur. J.*, 2010, **16**, 13773–13782.
33 S. C. Marker, S. N. MacMillan, W. R. Zipfel, Z. Li, P. C. Ford and J. J. Wilson, *Inorg. Chem.*, 2018, **57**, 1311–1331.
34 M. Schutte-Smith, S. C. Marker, J. J. Wilson and H. G. Visser, *Inorg. Chem.*, 2020, **59**, 15888–15897.
35 C.-C. Ko, A. W.-Y. Cheung, L. T.-L. Lo, J. W.-K. Siu, C.-O. Ng and S.-M. Yiu, *Coord. Chem. Rev.*, 2012, **256**, 1546–1555.
36 M. A. Wright and J. A. Wright, *Dalton Trans.*, 2016, **45**, 6801–6811.
37 M. R. Wasielewski, M. P. Niemczyk, W. A. Svec and E. B. Pewitt, *J. Am. Chem. Soc.*, 1985, **107**, 1080–1082.
38 Z. Deng, C. Li, S. Chen, Q. Zhou, Z. Xu, Z. Wang, H. Yao, H. Hirao and G. Zhu, *Chem. Sci.*, 2021, **12**, 6536–6542.
39 Z. Deng, N. Wang, Y. Liu, Z. Xu, Z. Wang, T.-C. Lau and G. Zhu, *J. Am. Chem. Soc.*, 2020, **142**, 7803–7812.
40 H. Yao, S. Chen, Z. Deng, M.-K. Tse, Y. Matsuda and G. Zhu, *Inorg. Chem.*, 2020, **59**, 11823–11833.
41 J. Karges, T. Yempala, M. Tharaud, D. Gibson and G. Gasser, *Angew. Chem., Int. Ed.*, 2020, **59**, 7069–7075.
42 Z. Wang, N. Wang, S.-C. Cheng, K. Xu, Z. Deng, S. Chen, Z. Xu, K. Xie, M.-K. Tse, P. Shi, H. Hirao, C.-C. Ko and G. Zhu, *Chem*, 2019, **5**, 3151–3165.
43 E. Petruzzella, J. P. Braude, J. R. Aldrich-Wright, V. Gandin and D. Gibson, *Angew. Chem., Int. Ed.*, 2017, **56**, 11539–11544.
44 B. T. Elie, J. Fernández-Gallardo, N. Curado, M. A. Cornejo, J. W. Ramos and M. Contel, *Eur. J. Med. Chem.*, 2019, **161**, 310–322.
45 B. T. Elie, Y. Pechenyy, F. Uddin and M. Contel, *J. Biol. Inorg. Chem.*, 2018, **23**, 399–411.
46 S. Parveen, M. Hanif, E. Leung, K. K. H. Tong, A. Yang, J. Astin, G. H. De Zoysa, T. R. Steel, D. Goodman, S. Movassaghi, T. Söhnel, V. Sarojini, S. M. F. Jamieson and C. G. Hartinger, *Chem. Commun.*, 2019, **55**, 12016–12019.

 